Published in final edited form as:
Exp Hematol. 2008 October ; 36(10): 1227–1235. doi:10.1016/j.exphem.2008.04.014.

Use of *Nramp2*-transfected Chinese hamster ovary cells and reticulocytes from *mk/mk* mice to study iron transport mechanisms

An-Sheng Zhang[a], **Francois Canonne-Hergaux**[b], **Samantha Gruenheid**[c], **Philippe Gros**[d], and **Prem Ponka**[e,f,g]

a*Department of Cell and Developmental Biology, Oregon Health and Science University, Portland, Ore., USA*

b*UPR 2301, CNRS, Gif-Sur-Yvette, France*

c*Department of Microbiology and Immunology, McGill University, Montreal, QC, Canada*

d*Department of Biochemistry, McGill University, Montreal, QC, Canada*

e*Department of Physiology, McGill University, Montreal, QC, Canada*

f*Department of Medicine, McGill University, Montreal, QC, Canada*

g*Lady Davis Institute for Medical Research, Jewish General Hospital Montreal, QC, Canada*

Abstract

Objective—We investigated mechanisms involved in iron (Fe) transport by DMT1 (endosomal Fe (II) exporter, encoded by the *Nramp2* gene) using wild-type Chinese hamster ovary (CHO) cells and *Nramp2*-transfected CHO cells, as well as reticulocytes from normal and *mk/mk* mice that have a defect in DMT1.

Materials and Methods—CHO cells and reticulocytes were incubated with ^{59}Fe bound to various ligands. The radioiron was present in its Fe(II) or Fe(III) forms or bound to transferrin (Tf), and the internalized ^{59}Fe measured under varying experimental conditions. Additionally, ^{125}I-Tf interaction with reticulocytes was investigated and ^{59}Fe incorporation into their heme was determined.

Results—Hyperexpression of DMT1 in CHO cells greatly increases their capacity to acquire ferrous iron. Although CHO-*Nramp2* cells showed an increase in Fe(III) uptake as compared to CHO cells, they transported Fe(III) with much lower efficacy than Fe(II). In addition to their defect in Fe uptake, *mk/mk* reticulocytes also showed a decrease in Tf receptor levels.

Conclusions—Given that CHO cells acquire iron from Fe(II)-ascorbate with much higher rates than from Fe(III)-Tf, Tf-receptor levels represent the rate-limiting step in their iron uptake. As Fe (III) transport by CHO-*Nramp2* cells can be inhibited by the impermeable oxidant $K_3Fe(CN)_6$, a membrane ferric reductase is probably needed for reduction of Fe(III) to Fe(II), which is then transported by DMT1. DMT1 is not a limiting factor in Fe acquisition by normal reticulocytes and their heme synthesis.

Virtually all organisms possess an absolute requirement for iron because of its unsurpassed catalytic versatility. However, the chemical properties of iron that allow for its usefulness are also responsible for its potential toxicity and, hence, iron metabolism is tightly controlled at

Offprint requests to: Prem Ponka, M.D., Ph.D., Lady Davis Institute for Medical Research, Jewish General Hospital, 3755 Cote Ste-Catherine Road, Montreal, QC, Canada H3T 1E2; E-mail: prem.ponka@mcgill.ca

both the organismal and cellular levels [1–4]. In vertebrates, iron is transported within the body between sites of absorption, storage, and utilization by the plasma glycoprotein transferrin [1] which binds ferric iron very tightly, but reversibly. Delivery of iron to most cells occurs following the binding of transferrin (Tf) to Tf receptors [5] on the cell membrane. Extracellular Fe_2^{3+}-Tf is bound by the membrane-bound Tf receptors and internalized via receptor-mediated endocytosis into an endosome. Iron is released from Tf following a decrease in endosomal pH (reviewed in [1]) and is then transported across the endosomal membrane by DMT1 [6,7]. DMT1 (also known as Nramp2, DCT1 {divalent cation transporter [8]} or Slc11a2), is encoded by a gene that belongs to the *"natural resistance macrophage-associated protein"* (*Nramp*)-family of genes identified by Gros and coworkers [9]. Mutations of *Nramp2* cause decreased iron uptake by erythroid cells (and possibly other cells) in mice with microcytic anemia (*mk/mk*) [6] and in anemic Belgrade (*b/b*) rats [7]. Additionally, several recent reports have demonstrated that DMT1 mutations cause hypochromic microcytic anemias in human patients [10–14]. Because the substrate for DMT1 is ferrous iron [8], reduction of Tf-borne Fe(III) must occur in endosomes. Importantly, Ohgami et al. [15] have recently identified a gene, *Steap3* (six transmembrane, epithelial antigen of the prostate 3), whose product is a compelling candidate for endosomal ferric reductase. The protein coded by this gene is highly expressed in hematopoietic tissues, is present in endosomes and colocalizes with Tf, Tf receptors, and DMT1.

Immature erythroid cells are the most avid consumers of iron, most of which is used for hemoglobin synthesis. Although normally all of this iron is delivered via the Tf receptor pathway [16], in vitro experiments revealed that immature erythroid cells can also acquire non-Tf-bound iron in its ferrous form [17,18]. It is likely that the transmembrane Fe^{2+} transport system in developing erythroid cells reflects the activity of DMT1. Physiologically, all iron in the circulation is Tf-bound and, hence, DMT1 expressed at the plasma membrane of erythroid and other cells has no substrate. Hence, in normal individuals DMT1 can assume its function of Fe^{2+}-transporter only following its recruitment into endosomes where it colocalizes with Tf [19,20].

In this study, we investigated the mechanisms involved in iron transport by DMT1, exploiting Chinese hamster ovary (CHO) cells transfected with mouse *Nramp2* gene as well as reticulocytes from wild-type and *mk/mk* mice. We found that hyperexpression of DMT1 in CHO cells dramatically increases their capacity to acquire ferrous iron. Although *Nramp2*-transfected CHO cells also display an increase in Fe(III) uptake, it is highly likely that the iron can be transported only following its reduction to Fe(II). Both wild-type *Nramp2*-transfected CHO cells and normal reticulocytes acquire Fe(II) at rates much higher than that at which iron is taken up physiologically from Tf. These observations suggest that Tf-receptor levels represent a limiting factor in iron uptake by all three cell types examined in this study. Reticulocytes from *mk/mk* mice show not only a defect in Fe(II) uptake, but also a decrease in iron uptake from Tf and a dramatic inhibition of iron incorporation into heme.

Materials and methods

Cells

CHO cells were transfected with mouse *Nramp2* gene as described by Gruenheid et al. [19]. Immunological staining using anti-DMT1 antibody demonstrated that transfected cells (referred to as CHO-*Nramp2* cells) exhibited a stable and high expression of DMT1 at the plasma membrane [19]. CHO cells were cultured in minimum essential medium containing 10% fetal calf serum at 37°C in a CO_2-incubator; medium for the growth of CHO-*Nramp2* cells was supplemented with 1 mg/mL G418.

Reticulocytosis was induced by injecting CD1 mice with neutralized phenylhydrazine (intraperitoneally) at a dose of 50 mg/kg/day for 3 continuous days. On the 3rd or 4th day following the last injection, blood was taken from the heart under ether anesthesia using heparin as anticoagulant, and red blood cells (−45% reticulocytes) were washed three times with ice-cold phosphatebuffered saline (PBS) at 4°C. Mature erythrocytes (containing virtually no reticulocytes) were obtained from untreated CD1 mice, by collecting the bottom quarter of packed red blood cells during the washing procedure.

In some experiments, untreated homozygous *mk/mk* mice (kindly provided by Dr. Mark Fleming, Harvard University) were used as a source of reticulocytes; control reticulocytes were collected from their heterozygous or wild-type (+/?) counterparts treated with phenylhydrazine as described here. In experiments comparing iron or Tf uptake by reticulocytes from *mk/mk* and +/? animals, a special effort was made to adjust concentration of reticulocytes in both samples to the same level. This was confirmed by measurement of RNA content [21] in reticulocyte samples from *mk/mk* and +/? animals.

^{59}Fe uptake by CHO cells

^{59}Fe(II) uptake—Reduction of ^{59}Fe(III) to ^{59}Fe(II) was accomplished using ascorbate as described by Egyed [17] using some modifications. Briefly, $^{56}FeSO_4$ (10-fold excess) was added to $^{59}FeCl_3$ in 0.1 M HCl (Amersham, UK), after which the ascorbate solution, deoxygenated by nitrogen gas, was added to make a final iron-to-ascorbate ratio of 1:44. After additional dilution with an appropriate incubation buffer, the ^{59}Fe(II)-ascorbate mixture was used (within 20 minutes) for uptake experiments. Using 1,10-phenanthroline and ferozine, that specifically bind Fe(II) to form spectrophotometrically detectable complexes, we demonstrated that iron remained reduced in the incubation buffer for at least 2 hours.

Preparation of CHO and CHO-Nramp2 cells for ^{59}Fe(II) uptake studies

Cells were collected following treatment with 0.25% trypsin, 1 mM ethylenediamine tetraacetic acid (GIBCO, Toronto, Ontario, Canada), and approximately 8×10^5 cells/well were seeded into six-well plates (Nunclon; VWR Canlab, Mississauga, Ontario, Canada). After about 16 hours preincubation in the medium described here, cells were washed twice with warm PBS, followed by addition of 2 mL deoxygenated warm incubation buffer (25 mM Tris, 25 mM Mes, 140 mM NaCl, 5.4 mM KCl, 5 mM glucose, 1.8 mM $CaCl_2$, pH 5.0 – 7.4) that was prepared as described by Fleming et al. [7], except that $MgSO_4$ was omitted; $MgSO_4$ was found to slightly inhibit Fe(II) uptake by CHO-*Nramp2* cells. After adding ^{59}Fe(II)-ascorbate at the indicated concentrations, the uptake was initiated by immediately transferring the plates to the CO_2 incubator (37°C), with gentle shaking for 10 minutes. The ^{59}Fe uptake was terminated by three washes with ice-cold PBS. Cells were detached and the membrane-associated ^{59}Fe was removed using 30-minute incubation (4°C) in 2 mL PBS containing 1 mg/mL pronase plus 5 mM ethylenediamine tetraacetic acid [22]. After an additional two washes with PBS, the ^{59}Fe radioactivities in both cell pellets and supernatants were counted using 1282 Compugamma gamma counter (LKB Instruments, Pleasant Hill, CA, USA). The former represented intracellular ^{59}Fe, while the latter accounted for the membrane-bound ^{59}Fe. As no significant difference in either cell number or protein contents was observed between CHO and CHO-*Nramp2* cells after 16 hours of preincubation, calculations for Fe uptake were based on the cell numbers at the time of seeding, and expressed as pmole Fe/10^6 cels. All ^{59}Fe uptake measurements were performed in duplicates; initial control experiments revealed that the ^{59}Fe uptake at 4°C was negligible.

Non-Tf ^{59}Fe(III) uptake

^{59}Fe(III)-citrate (ratio of 1:100) was prepared as described previously [22] and ^{59}Fe(III) uptake experiments were conducted as described for ^{59}Fe(II) uptake studies.

^{59}Fe uptake from ^{59}Fe-Tf

$^{59}Fe_2$-Tf was prepared as described by Martinez-Medellin and Schulman [23]. ^{59}Fe uptake was performed (CO_2-incubator, 37°C) in minimum essential medium supplemented with 25 mM HEPES (pH 7.4), 10 mM $NaHCO_3$, and 1% bovine serum albumin, either in the presence of different concentrations of $^{59}Fe_2$-Tf for 1 hour or in the presence of 2.5 μM $^{59}Fe_2$-Tf for different time intervals. The ^{59}Fe uptake was terminated by washing cells (three times) with ice-cold PBS. Membrane-associated ^{59}Fe-Tf was removed by pronase (1 mg/mL) treatment (30 minutes/4°C) after which the cells were collected and washed twice with icecold PBS. The radioactivity in cell pellets was counted and the rates of iron uptake expressed as pmoles per 10^6 cells.

In some experiments intracellular ^{59}Fe distribution in CHO cells, following their incubation with either ^{59}Fe(II)-ascorbate or $^{59}Fe_2$-Tf, was examined. Lysates of CHO cells were metabolically labeled with ^{59}Fe, separated on 3% to 20% polyacrylamide gradient gels in the presence of Triton X-100 and ^{59}Fe was detected by autoradiography as previously described [24,25]. Briefly, the cell pellet was resuspended in 80 μL lysing solution containing 0.14 M NaCl, 0.1 M HEPES, 1.5% Triton X-100, and 1 mM phenylmethylsulfonyl fluoride (pH 7.4) at 4°C. After vigorous vortexing, the lysates were centrifuged using a microcentrifuge for 15 minutes (4°C). The supernatants (Triton X-100 soluble) were carefully transferred into clean tubes. The ^{59}Fe radioactivities in both the supernatant and pellet (Triton X-100 insoluble) fractions were counted for ^{59}Fe radioactivity. The total supernatants were subjected to gradient gel electrophoresis, after which the gel was dried and autoradiographed, the ^{59}Fe-containing bands cut, and their ^{59}Fe radioactivities measured using a gamma counter. Human $^{59}Fe_2$-Tf and murine-^{59}Fe ferritin were used as markers and included in the gel in separate lanes. Following the autoradiography, three ^{59}Fe-containing bands could be distinguished; two of them comigrated with ^{59}Fe-Tf and ^{59}Fe-ferritin markers, respectively. Moreover, the identities of ^{59}Fe-Tf and ^{59}Fe-ferritin were confirmed by supershifts of their respective bands using anti-Tf or anti-ferritin antibodies. In addition, ^{59}Fe-radioactivity was also found in a diffuse rapidly migrating band, corresponding to Y-band identified previously in reticulocytes treated with heme synthesis inhibitors [24]; when desferrioxamine was added to the samples before electrophoresis, most of the ^{59}Fe radioactivity found in the rapidly migrating band Y disappeared.

^{59}Fe uptake by reticulocytes and erythrocytes

^{59}Fe(II) uptake was measured using ^{59}Fe(II)-ascorbate (see above) added to a suspension of erythrocytes or reticulocytes (hematocrit −20%) in buffer containing 270 mM sucrose, 4 mM Pipes (pH 4.5 – 7.4) [26].

^{59}Fe uptake from ^{59}Fe-Tf was measured by incubating cells (hematocrit −20%) in minimum essential medium containing 25 mM HEPES (pH 7.4), 10 mM $NaHCO_3$ and 1% bovine serum albumin. At indicated time intervals, cells were thoroughly washed in ice-cold PBS and total cell ^{59}Fe-radioactivity counted. ^{59}Fe incorporated into heme was measured following heme extraction from ^{59}Fe-labeled cells using acid methyl ethyl ketone [27].

^{125}I-Tf cycle in reticulocytes

Iron-saturated ^{125}I-Tf was prepared using Iodo-Bead (Pierce, Rockford, IL, USA) according to manufacturer's procedure. Iron-saturated Tf and Na^{125}I were obtained from Sigma (St Louis,

MO, USA) and ICN Biomedical (Irving, CA, USA), respectively. The rates of cell surface-associated ^{125}I-Tf internalization were measured by incubation of reticulocytes in presence of 2 μM ^{125}I-Tf at 37°C in the same buffer used for ^{59}Fe uptake studies. Samples were taken at different time intervals and immediately transferred into ice-cold PBS to terminate the uptake. After three washes, cell pellets (50 μL) were resuspended in 400 μL 0.25% pronase and incubated at 4°C for 30 minutes to remove the membrane-associated ^{125}I-Tf. ^{125}I-Tf radioactivity in the washed cells represented internalized fraction.

To measure intracellular^{125}I-Tf release, reticulocytes were first incubated in the presence of 2 μM of ^{125}I-Tf at 37°C for 30 minutes. Following three washes with ice-cold PBS at 4°C to eliminate non–cell-associated ^{125}I-Tf, cell pellets were resuspended in the buffer supplemented with 2 μM ^{56}Fe-Tf. The intracellular ^{125}I-Tf release was initiated by warming up the samples at 37°C. Samples were taken at different time intervals and immediately transferred into ice-cold PBS to terminate the release. After centrifugation, the ^{125}I-Tf radioactivities were measured in both cell pellets and supernatant that contained released ^{125}I-Tf.

Scatchard analysis of ^{125}I-Tf binding to TfR was performed as described previously [28]. Briefly, reticulocytes were incubated in the presence of increasing concentrations of ^{125}I-Tf for 2 hours, followed by three washed with ice-cold PBS to remove the unbound ^{125}I-Tf. The radioactivity in cell pellet represented the fraction of cell surface Tf receptor-associated ^{125}I-Tf. The nonspecific binding was obtained in the presence of 50-fold excess of $^{56}Fe_2$-Tf.

Data analysis

For all data herein, the average of duplicate samples is presented; differences in duplicate samples were <5%. Each experiment was repeated at least three times and representative results are presented. “Day-to-day” variability and logistical constraints generally precluded sophisticated statistical analysis; however, the deviation in relative changes between replicate experiments was typically <3%.

Results

Fe(II) uptake by CHO cells

As Fe(II) transport via DMT1 is coupled with proton transport [8], we examined the effect of pH on ^{59}Fe(II) uptake by CHO-*Nramp2* cells and CHO cells. Figure 1A shows that in the pH ranging from 5.0 to 7.4, CHO-*Nramp2* cells, as compared to wild-type CHO cells, exhibit considerably higher uptake of ^{59}Fe(II). The rate of Fe(II) uptake by CHO-*Nramp2* cells is highest at pH 5.5, and at this pH the cells take up about 15-fold more Fe(II) than their untransfected counterparts (Fig. 1A). In both cell types the uptake of Fe(II) is saturable at about 10 μM iron, at which concentration the CHO-*Nramp2* cells take up 12.5-fold more Fe(II) than the CHO cells (Fig. 1B). At both saturating and lower concentrations of Fe(II), its uptake by both CHO and CHO-*Nramp2* cells is linear for at least 60 minutes (Table 1).

Fe(II) uptake by both CHO and CHO-*Nramp2* cells is temperature-dependent since incubation at 4°C inhibited the uptake by >97%. Incubation of cells in the presence of rotenone (10 μM) inhibited Fe(II) uptake by CHO-*Nramp2* cells by >70%, indicating that Fe(II) transport via DMT1 is an adenosine triphosphate-dependent process (not shown).

As DMT1 expressed in oocytes seems to transport not only Fe^{2+}, but also numerous other divalent metal ions [8], we next investigated the effects of other metals on ^{59}Fe(II) uptake by CHO-*Nramp2* cells. Table 2 shows that a variety of divalent metals interfere with ferrous iron uptake by CHO-*Nramp2* cells and the order of their inhibitory effects is as follows: Cu > Cd > Co > Mn > Ni. These results confirm that DMT1 displays a broad substrate selectivity [8]. However, we did not observe any significant inhibitory effect of Zn^{2+} and Pb^{2+} on ferrous iron

uptake by CHO-*Nramp2*. This finding is in conflict with the observation of Gunshin et al. [8], who reported that DCT1/ DMT1 mediates cellular uptake of Zn^{2+} and Pb^{2+}. Although some divalent metals (Cd^{2+}, Co^{2+}, Mn^{2+}) inhibited ferrous iron uptake by nontransfected CHO cells, Cu^{2+}, Ni^{2+}, Mg^{2+}, and Zn^{2+} did not inhibit this process (Table 2); however, Cu^{2+}, at 5 μM and higher concentrations, inhibited ferrous iron uptake by CHO-*Nramp2* cells. Even more surprisingly, Cu^{2+} and Pb^{2+} stimulated Fe(II) uptake by nontransfected CHO cells (Table 2). It is possible that CHO cells, similarly as immature erythroid cells [26], have two ferrous iron transport systems one of which is represented by DMT1. The second Fe(II) transport system in erythroid cells becomes prominent at higher iron concentrations and is stimulated by KCl, PbCl, LiCl, and CsCl [26]. Experiments are being planned to investigate whether DMT1-independent transport system can account for Pb^{2+}-induced stimulation of Fe(II) uptake by CHO cells.

Fe(III) uptake by CHO cells

In the next set of experiments, we investigated whether a high expression of DMT1 in CHO cells affects the rate of Fe(III) uptake. Figure 2 demonstrates that Fe(III) uptake, as compared to Fe(II) uptake, exhibits some similarities but also several remarkable differences. Fe(III) uptake by CHO-*Nramp2* is higher than that by CHO cells and shows pH dependency, although the maximum uptake occurs at pH as low as 4.5 (Fig. 2A). Fe(III) uptake by both cell lines is saturable at about 10 μM iron concentration (Fig. 2B). However, the quantitative difference between Fe(III) uptake in *Nramp2*-transfected vs wild-type CHO cells is less prominent than is the case for Fe(II) uptake. Even more importantly, the ratio of Fe(II):Fe(III) uptake by CHO-*Nramp2* cells is 57 and 40 at pH 5.5 and 7.4, respectively (compare Fig. 1A and Fig. 2A), indicating that Fe(III) is transported with much lower efficacy.

Fe(III) uptake is temperature-dependent (not shown) as well as adenosine triphosphate-dependent because it can be inhibited by rotenone (Table 3). Importantly, potassium ferricyanide ($K_3Fe(CN)_6$), in concentrations as low as 1 μM, causes 70% inhibition of Fe(III) uptake by CHO-*Nramp2* cells (Table 3), decreasing the uptake almost to the level seen in wild-type CHO cells. In a control experiment, KCN (1 mM) had virtually no effect on Fe(III) uptake (not shown). Potassium ferricyanide serves as an extracellular “electron sink” and is known to inhibit a membrane ferric-reductase [29,30]. We conclude that DMT1 can transport Fe(III) only following its reduction to Fe(II), a process likely to be mediated by the plasma membrane ferric reductase inhibitable by $K_3Fe(CN)_6$. Cu^{2+} significantly inhibited, and ascorbate dramatically stimulated, Fe(III) uptake by both cell lines (Table 3), providing further support for the idea that reduction of iron is necessary and that DMT1 is involved in the transport.

Tf-derived Fe uptake by CHO cells

As expected, both CHO and CHO-*Nramp2* cells were capable of acquiring ^{59}Fe from $^{59}Fe_2$-Tf by a temperature- and energy-dependent process, and the uptake of ^{59}Fe was linear for at least 3 hours (not shown). CHO and CHO-*Nramp2* cells took up Tf-borne iron with identical rates, leading to the accumulation of approximately 13 pmoles Fe/10^6 cells during a 1-hour incubation at pH 7.4 (Table 4).

Figure 3 shows that about 80% of ^{59}Fe taken up by wildtype CHO cells, following 1-hour incubation with ^{59}Fe-Tf, can be found in a Triton X-100–soluble fraction, 10% of which appears in ferritin. On the other hand, after 1-hour incubation of CHO-*Nramp2* cells with ^{59}Fe(II)-ascorbate, only 45% of ^{59}Fe is in Triton X-100-soluble fraction, and 2% of this ^{59}Fe appears in ferritin; the vast majority of ^{59}Fe is found in an as yet unidentified fraction with fast mobility upon native electrophoresis [24,25]; ^{59}Fe in this fraction can be readily chelated by desferrioxamine.

Fe uptake by mouse reticulocytes and erythrocytes

As expected (Table 5), mature erythrocytes are unable to take up iron from Tf, but they have some, though very limited, capacity to incorporate ^{59}Fe from ^{59}Fe(II)-ascorbate. As compared to erythrocytes, reticulocytes take up ferrous iron (likely via DMT1) with about a 14-fold higher efficiency. Reticulocytes acquire iron from ferrous-ascorbate much more efficiently (eightfold) than from Fe_2-Tf. Most (86%) of Tf-borne iron is used for heme synthesis, whereas only 8% of the iron derived from Fe(II)-ascorbate appears in heme (Table 5). Even more importantly, absolute amount of iron used for heme synthesis is about 30% lower when the cells are offered non-Tf, Fe(II), as a substrate (Table 5).

Fe(II) uptake by normal reticulocytes follows a pattern of pH-dependency, with a maximumuptake at pH 7 (Fig. 4) that is different from that described for CHO-*Nramp2* cells (Fig. 1A). However, it should be noted that CHO-*Nramp2* cells were incubated in a buffer containing only salt that caused hemolysis of reticulocytes below pH 7. Therefore, for ferrous uptake studies, reticulocytes were incubated in a buffer containing a high concentration of sucrose [26] that did not cause hemolysis. Figure 4 shows that reticulocytes derived from *mk/mk* mice exhibited a significant decrease in their capacity to acquire ferrous iron, and the uptake decreased progressively with decreasing pH.

Reticulocytes from *mk/mk* mice, as compared to those from +/? animals, show about a 70% lower rate of iron uptake from Tf and use iron for heme synthesis less efficiently; after a 1-hour incubation wild-type reticulocytes used about 90% ^{59}Fe for heme synthesis while reticulocytes from *mk/mk* mice used only about 65% (Fig. 5). Experiments were next designed to investigate whether the decrease in iron uptake from Tf by *mk/mk* reticulocytes could be accounted for only by defective DMT1 [6] or whether the reticulocytes from *mk/mk* animals had additional defects. We examined the rate of ^{125}I-Tf internalization, ^{125}I-Tf release and the affinity of Tf to Tf receptors and found no difference in these parameters in reticulocytes from *mk/mk* mice as compared to those from +/? animals (not shown). However, we unexpectedly found that the amount of ^{125}I-Tf bound to surface receptors in reticulocytes from mk/mk mice was significantly reduced (Fig. 6), suggesting either an overall decrease in Tf receptor levels or a decrease in the presence of receptors at the cell surface.

Discussion

DMT1 has recently been identified as the first transmembrane iron transporter [3,4,6–8]. It plays a dual role in transporting inorganic iron across the apical membrane of enterocytes as well as in translocating Tf-derived iron through endosomal membrane. In the first part of this study we investigated the uptake of iron from various sources by wild-type CHO cells and those expressing high levels of DMT1 in order to further characterize this transporter's function and evaluate its involvement in overall cellular iron metabolism.

We have demonstrated that DMT1 efficiently transports ferrous iron into the cells that express high levels of this protein. The transport is temperature-, energy-, and pH-dependent. The highest iron-transporting activity occurs at pH 5.5, which is the pH needed for iron release from Tf in endosomes. These results corroborate previous findings of Gunshin et al. [8]. We also confirmed that several divalent metals (Cu, Cd, Co, Mn, Ni) are likely to be transported by DMT1 because they inhibit its Fe(II)-transporting activity. However, in contrast with the earlier report [8], we did not find inhibition of Fe(II) uptake by CHO-*Nramp2* cells in the presence of Zn^{2+} and Pb^{2+}. This discrepancy suggests that cell-specific factors (oocytes, ref. [8] or CHO cells, this study) may modulate the transport function of DMT1.

We also compared CHO cells and CHO-*Nramp2* cells for their capacity to take up Fe(III) from ferric citrate. Somewhat surprisingly, we demonstrated that CHO-*Nramp2* cells, as compared

to their untransfected counterparts, have about fivefold higher uptake of iron offered in its ferric form. However, it is highly unlikely that DMT1 transports Fe(III) directly, and this conclusion is based on the following observations: Ferric iron transport by CHO-*Nramp2* cells can be inhibited by the impermeable oxidant potassium ferricyanide, that inhibits the plasma membrane ferric reductase [29,30]. This result strongly suggests that Fe(III) has to be first reduced to Fe(II), which can then be transported by DMT1. Additionally, Cu^{2+}, which inhibits Fe(II) transport by DMT1, significantly inhibits iron uptake (offered as ferric-citrate) by CHO-*Nramp2* cells. It is possible that at least some ferric iron, taken up by CHO-*Nramp2* cells, is reduced by Steap3; although most of this protein is localized intracellularly, a small fraction of Steap3 appears on the plasma membranes (Dr. Mark Fleming, personal communication). However, it is unknown whether this reductase is inhibitable by ferricyanide. In any case, these results are relevant to the mechanism of tissue iron uptake of non–transferrin-bound iron that is present in plasma of patients with severe iron overload [31–33].

Importantly, CHO and CHO-*Nramp2* cells take up iron from Tf with identical rates (Table 4) that are much lower than the rates with which these cells take up ferrous iron (Fig. 1). These results strongly indicate that iron-transporting capacity of DMT1, even in wild-type CHO cells, greatly exceeds the iron-transporting capacity of the Tf-receptor pathway. In other words, Tf-receptor levels represent the rate-limiting step in iron uptake via the physiological Tf-dependent pathway. Moreover, intracellular ^{59}Fe distribution is grossly disturbed when ^{59}Fe is offered in the form of ^{59}Fe(II)-ascorbate, in particular in CHO-*Nramp2* cells (Fig. 3). About 85% of ^{59}Fe taken up (60 minutes) from $^{59}Fe_2$-Tf by wild-type CHO cells can be recovered in the Triton X-100–soluble fraction. However, CHO-*Nramp2* cells following their incubation (60 minutes) with ^{59}Fe(II)-ascorbate contain only 45% of their ^{59}Fe in a Triton X100-soluble fraction, most of which (95%) can be found in the ill-defined fraction Y [24,25] with a high mobility following polyacrylamide gel electrophoresis (Fig. 3). In CHO-*Nramp2* cells, provided with ^{59}Fe(II), radioiron probably accumulates in this fraction, since the uptake of iron greatly exceeded the iron-storing capacity of ferritin; as compared with CHO cells, CHO-*Nramp2* cells supplied with ^{59}Fe(II) show a 6.5-fold increase of ^{59}Fe-radioactivity in the fraction Y, but only a twofold increase in ferritin (Fig. 3).

In the second part of this study we examined uptake of iron, using either Fe_2-Tf or Fe(II)-ascorbate as sources, by reticulocytes obtained from wild-type or *mk/mk* mice. Reticulocytes, as compared to mature erythrocytes, take up ferrous iron with about 15-fold higher efficacy, suggesting that DMT1 either disappears or becomes inactive with reticulocyte maturation (Fig. 4). Although reticulocytes can incorporate some ^{59}Fe into heme when incubated with ^{59}Fe(II)-ascorbate, the efficiency with which they utilize for heme synthesis ^{59}Fe derived from $^{59}Fe_2$-Tf, is significantly higher. This indicates that the Tf-receptor pathway plays an important role in the efficient targeting of iron towards mitochondria. As is the case with CHO cells, levels of Tf receptors in reticulocytes seem to represent the rate-limiting step in iron acquisition from Tf because the maximum iron uptake from Fe(II)-ascorbate is about eightfold higher than that from Fe_2-Tf.

As expected [6,34] reticulocytes from *mk/mk* mice, as compared to those from normal mice, exhibit a defect in Fe(II) uptake that is most prominent at pH 6. The decrease is so dramatic that it could produce a limiting step for iron uptake via the Tf-receptor pathway. In fact, iron uptake from Tf is also dramatically decreased in reticulocytes from *mk/mk* mice (Fig. 5), but the decreased DMT1 activity is probably not the only factor responsible for this defect. Our finding of lower cell surface binding of ^{125}I-Tf (Fig. 6), suggests that there may be a decrease in total Tf receptors levels in these mice. This would be consistent with our previous finding that inhibitors of heme synthesis decrease Tf receptor expression in induced murine erythroleukemia cells [35]. However, Garrick et al. have previously shown an increase in Tf receptor levels in reticulocytes from Belgrade rats [28]. Further evidence is needed to determine

whether the total levels of Tf receptors are indeed decreased in *mk/mk* reticulocytes or if there is another cause for our observation of decreased surface Tf binding, such as retention of a subpopulation of noncycling Tf receptors within the cells.

Acknowledgments

Supported by grants from Canadian Institutes of Health Research (MT-14100) (to PP), the National Institutes of Health grant DK080765 (to A–S Z) and the National Institute of Allergy and Infections Diseases grant (AI 35327) (to P.G.). P.G. is a Senior Scientist of Canadian Institutes of Health Research. The authors thank Sandy Fraiberg for excellent editorial assistance and Dr. Alex Sheftel and Shan Soe-Lin for helpful comments.

References

1. Richardson DR, Ponka P. The molecular mechanisms of the metabolism and transport of iron in normal and neoplastic cells. Biochim Biophys Acta 1997;1331:1–40. [PubMed: 9325434]
2. Eaton JW, Qian M. Molecular bases of cellular iron toxicity. Free Radic Biol Med 2002;32:833–840. [PubMed: 11978485]
3. Hentze MW, Muckenthaler MU, Andrews NC. Balancing acts: molecular control of mammalian iron metabolism. Cell 2004;117:285–297. [PubMed: 15109490]
4. De Domenico I, McVey Ward D, Kaplan J. Regulation of iron acquisition and storage: consequences for iron-linked disorders. Nat Rev Mol Cell Biol 2008;9:72–81. [PubMed: 17987043]
5. Ponka P, Lok CN. The transferrin receptor: role in health and disease. Int J Biochem Cell Biol 1999;31:1111–1137. [PubMed: 10582342]
6. Fleming MD, Trencor CC 3rd, Su MA, et al. cytic anaemia mice have a mutation in Nramp2, a candidate iron transporter gene. Nat Genet 1997;16:383–386. [PubMed: 9241278]
7. Fleming MD, Romano MA, Su MA, Garrick LM, Garrick MD, Andrews NC. Nramp2 is mutated in the anemic Belgrade (b) rat: evidence of a role for Nramp2 in endosomal iron transport. Proc Natl Acad Sci U S A 1998;95:1148–1153. [PubMed: 9448300]
8. Gunshin H, Mackenzie B, Berger UV, et al. Cloning and characterization of a mammalian proton-coupled metal-ion transporter. Nature 1997;388:482–488. [PubMed: 9242408]
9. Cellier M, Prive G, Belouchi A, et al. Nramp defines a family of membrane proteins. Proc Natl Acad Sci U S A 1995;92:10089–10093. [PubMed: 7479731]
10. Mims MP, Guan Y, Pospisilova D, et al. Identification of a human mutation of DMT1 in a patient with microcytic anemia and iron overload. Blood 2005;105:1337–1342. [PubMed: 15459009]
11. Priwitzerova M, Nie G, Sheftel AD, Pospisilova D, Divoky V, Ponka P. Functional consequences of the human DMT1 (SLC11A2) mutation on protein expression and iron uptake. Blood 2005;106:3985–3987. [PubMed: 16091455]
12. Iolascon A, d'Apolito M, Servedio V, Cimmino F, Piga A, Camaschella C. Microcytic anemia and hepatic iron overload in a child with compound heterozygous mutations in DMT1 (SCL11A2). Blood 2006;107:349–354. [PubMed: 16160008]
13. Beaumont C, Delaunay J, Hetet G, Grandchamp B, de Montalembert M, Tchernia G. Two new human DMT1 gene mutations in a patient with microcytic anemia, low ferritinemia, and liver iron overload. Blood 2006;107:4168–4170. [PubMed: 16439678]
14. Iolascon A, Camaschella C, Pospisilova D, Piscopo C, Tchernia G, Beaumont C. Natural history of recessive inheritance of DMT1 mutations. J Pediatr 2008;152:136–139. [PubMed: 18154916]
15. Ohgami RS, Campagna DR, Greer EL, et al. Identification of a ferri reductase required for efficient transferrin-dependent iron uptake on erythroid cells. Nat Genet 2005;37:1264–1269. [PubMed: 16227996]
16. Ponka P. Tissue-specific regulation of iron metabolism ad heme synthesis: distinct control mechanisms in erythroid cells. Blood 1997;89:1–25. [PubMed: 8978272]
17. Egyed A. Carrier mediated iron transport through erythroid cell membrane. Br J Haematol 1988;68:483–486. [PubMed: 3377990]
18. Morgan EH. Membrane transport of non-transferrin-bound iron by reticulocytes. Biochim Biophys Acta 1988;943:428–439. [PubMed: 3415985]

19. Gruenheid S, Canonne-Hergaux F, Gauthier S, Hackam DJ, Grinstein S, Gros P. The iron transport protein Nramp2 is an integral membrane glycoprotein that colocalizes with transferrin in recycling endosomes. J Exp Med 1999;189:831–841. [PubMed: 10049947]
20. Canonne-Hergaux F, Zhang AS, Ponka P, Gros P. Characterization of the iron transporter DMT1 (NRAMP2/DCT1) in red blood cells of normal and anemic mk/mk mice. Blood 2001;98:3823–3830. [PubMed: 11739192]
21. Schneider WC. Determination of nucleic acids in tissues by pentose analysis. Methods Enzymol 1957;3:680–684.
22. Graham RM, Morgan EH, Baker E. Ferric citrate uptake by cultured rat hepatocytes is inhibited in the presence of transferrin. Eur J Biochem 1998;253:139–145. [PubMed: 9578471]
23. Martinez-Medellin J, Schulman HM. The kinetics of iron and transferring incorporation into rabbit erythroid cells and the nature of stromal-bound iron. Biochim Biophys Acta 1972;264:272–274. [PubMed: 5028505]
24. Richardson DR, Ponka P, Vyoral D. Distribution of iron in reticulocytes after inhibition of heme synthesis with succinylacetone: examination of the intermediates involved in iron metabolism. Blood 1996;87:3477–3488. [PubMed: 8605367]
25. Vyoral D, Petrak J, Hradilek A. Separation of cellular iron containing compounds by electrophoresis. Biol Trace Elem Res 1998;61:263–275. [PubMed: 9533565]
26. Hodgson LL, Quail EA, Morgan EH. Iron transport mechanisms in reticulocytes and mature erythrocytes. J Cell Physiol 1995;162:181–190. [PubMed: 7822429]
27. Teale FW. Cleavage of the haem-protein link by acid methyl-ketones. Biochim Biophys Acta 1959;35:543. [PubMed: 13837237]
28. Garrick MD, Gniecko K, Liu Y, Cohan DS, Garrick LM. Transferrin and the transferrin cycle in Belgrade rat reticulocytes. J Biol Chem 1993;268:14867–14874. [PubMed: 8325865]
29. Sun IL, Navas P, Crane FL, Morre DJ, Low H. NADH diferric transferring reductase in liver plasma membrane. J Biol Chem 1987;262:15915–15921. [PubMed: 3680232]
30. Sun IL, Crane FL, Grebing C, Low H. Properties of a transplasma membrane electron transport system in HeLa cells. J Bioenerg Biomembr 1984;16:583–595. [PubMed: 6537437]
31. Hershko C, Graham G, Bates GW, Rachmilewitz EA. Non-specific serum iron in thalassaemia: an abnormal serum iron fraction of potential toxicity. Br J Haematol 1978;40:255–263. [PubMed: 708645]
32. Brissot P, Loréal O. Role of non-transferrin-bound iron in the pathogenesis of iron overload and toxicity. Adv Exp Med Biol 2002;509:45–53. [PubMed: 12572988]
33. Cabantchik ZI, Breuer W, Zanninelli G, Cianciulli P. LPI-labile plasma iron in iron overload. Best Pract Res Clin Haematol 2005;18:277–287. [PubMed: 15737890]
34. Su MA, Trenor CC, Fleming JC, Fleming MD, Andrews NC. The G185R mutation disrupts function of the iron transporter Nramp2. Blood 1998;92:2157–2163. [PubMed: 9731075]
35. Chan RY, Seiser C, Schulman HM, Kuhn LC, Ponka P. Regulation of transferrin receptor mRNA expression. Distinct regulatory features in erythroid cells. Eur J Biochem 1994;220:683–692. [PubMed: 8143723]

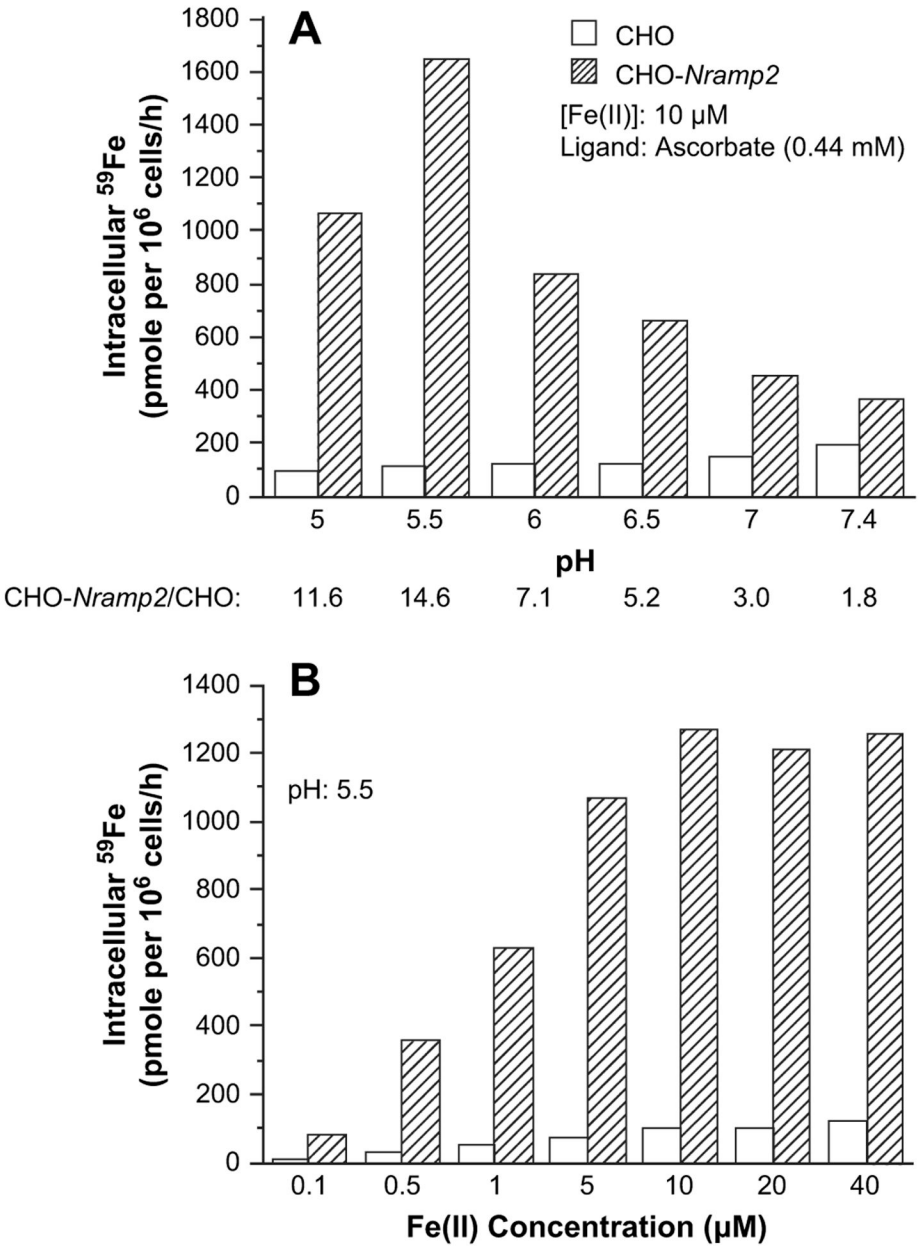

Figure 1.

Ferrous iron uptake by Chinese hamster ovary (CHO) and CHO-*Nramp2* cells. (**A**) pH-dependent uptake of Fe(II). (**B**) Concentration-dependent uptake of Fe(II).

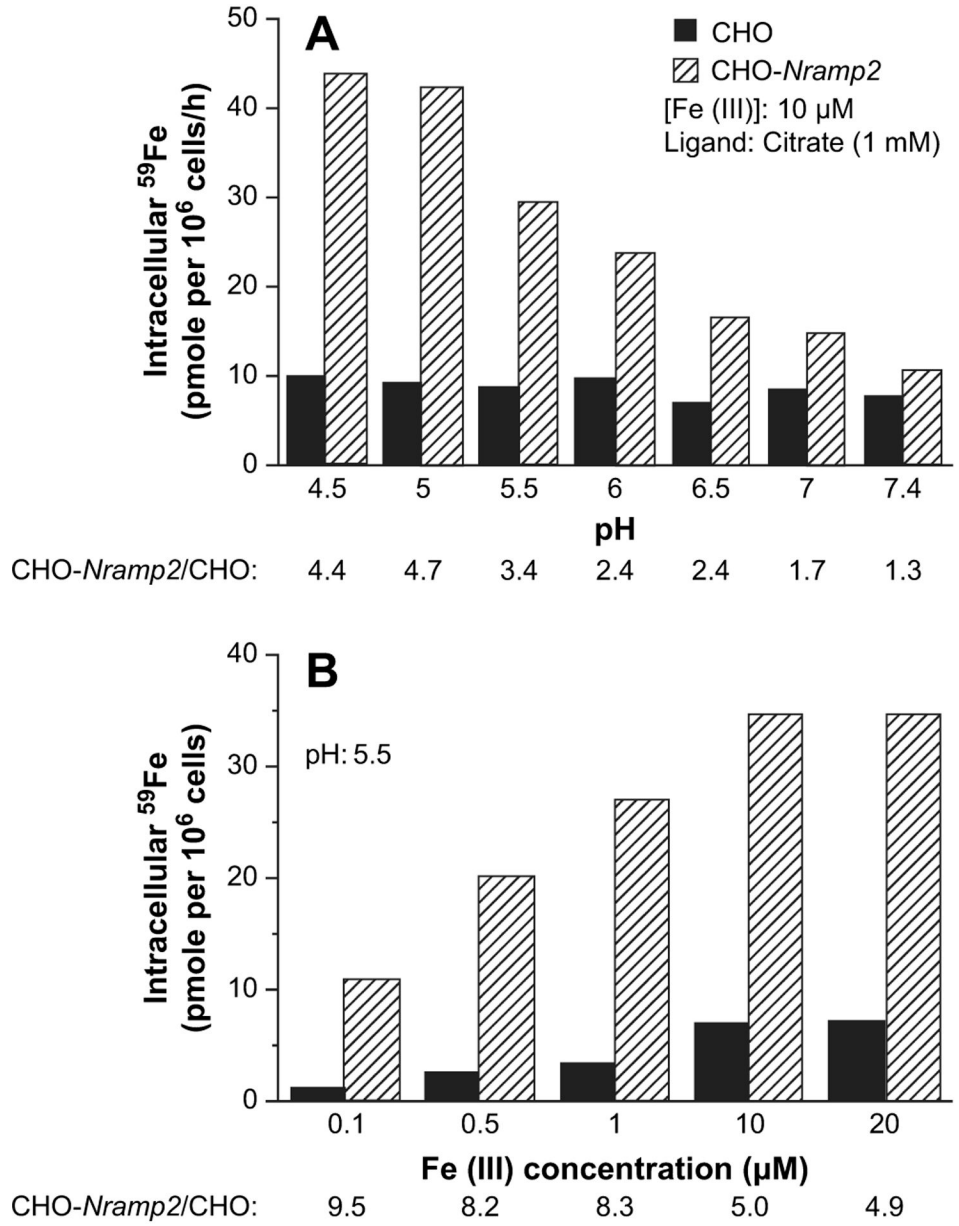

Figure 2.
Ferric iron uptake by Chinese hamster ovary (CHO) and CHO-*Nramp2* cells. (**A**) pH-dependent uptake of Fe(III). (**B**) Concentration-dependent uptake of Fe(III).

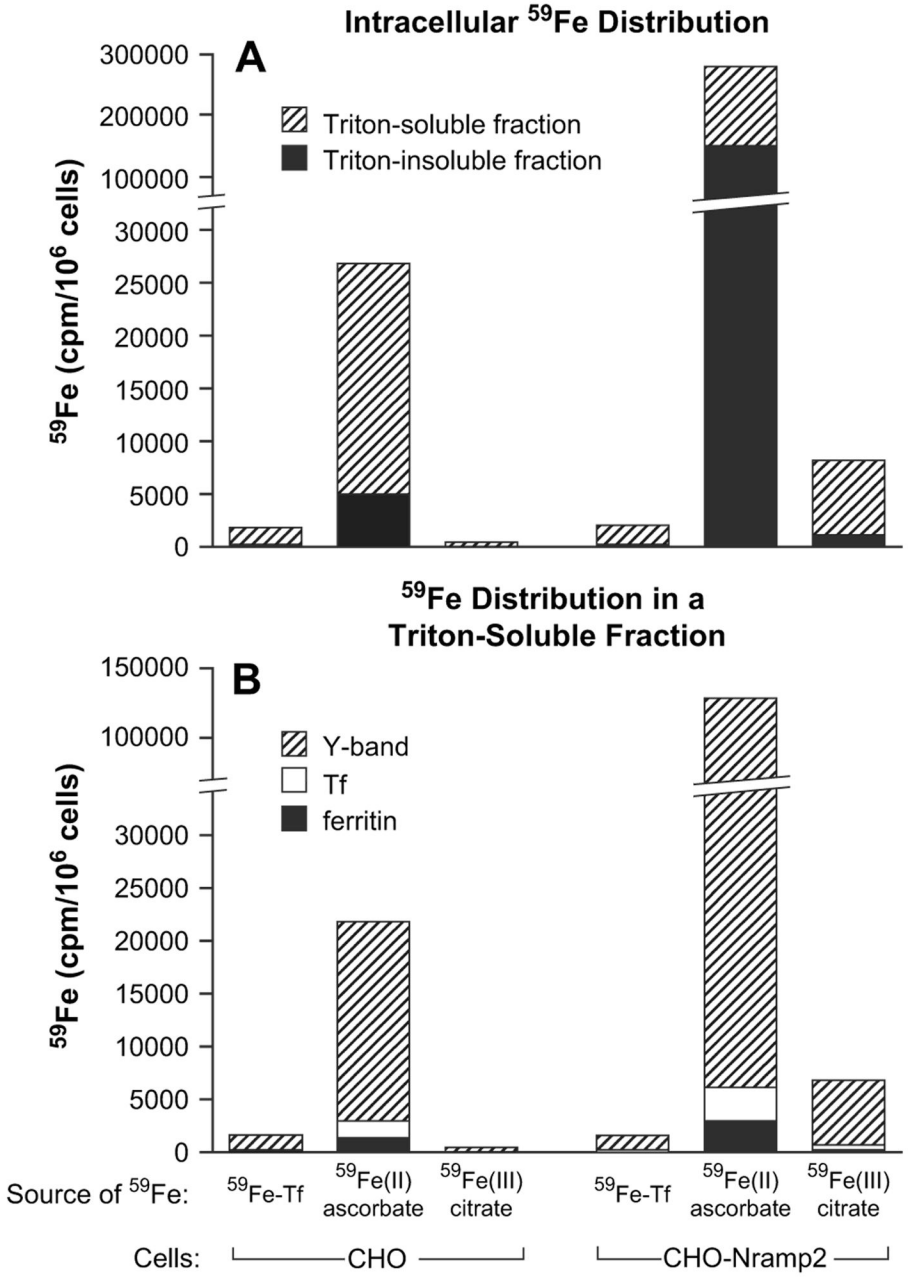

Figure 3.

^{59}Fe distribution in Chinese hamster ovary (CHO) or CHO-*Nramp2* cells incubated with various sources of iron. Cells were incubated with $^{59}Fe_2$-transferrin (Tf) (5 μM), ^{59}Fe(II)-ascorbate (10 μM) or ^{59}FeIII)-citrate (10 μM) for 1 hour, washed, and cell pellets solubilized as described in Materials and Methods. ^{59}Fe radioactivity was measured in Triton X- 100 insoluble and soluble fractions (**A**), following which soluble fractions were subjected to native gradient gel electrophoresis and the ^{59}Fe radioactivity in Y-band, Tf and ferritin (**B**) measured as described in Materials and Methods.

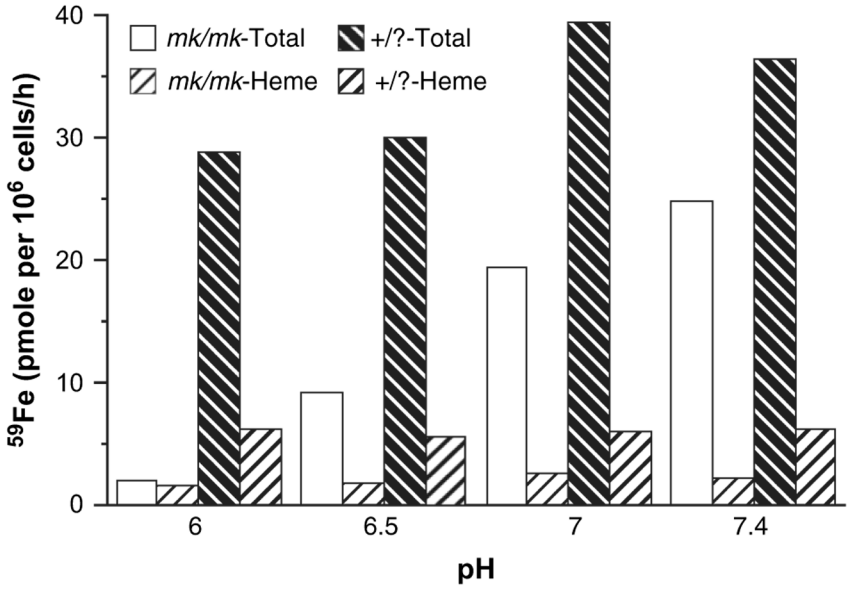

Figure 4.

^{59}Fe(II) uptake by reticulocytes obtained from *mk/mk* and +/? reticulocytes. The cells were incubated with 59Fe(II)-ascorbate (20 μM and 0.88 mM, respectively) for 60 minutes at 37° C. ^{59}Fe-heme was extracted using acid methyl ethyl ketone [27].

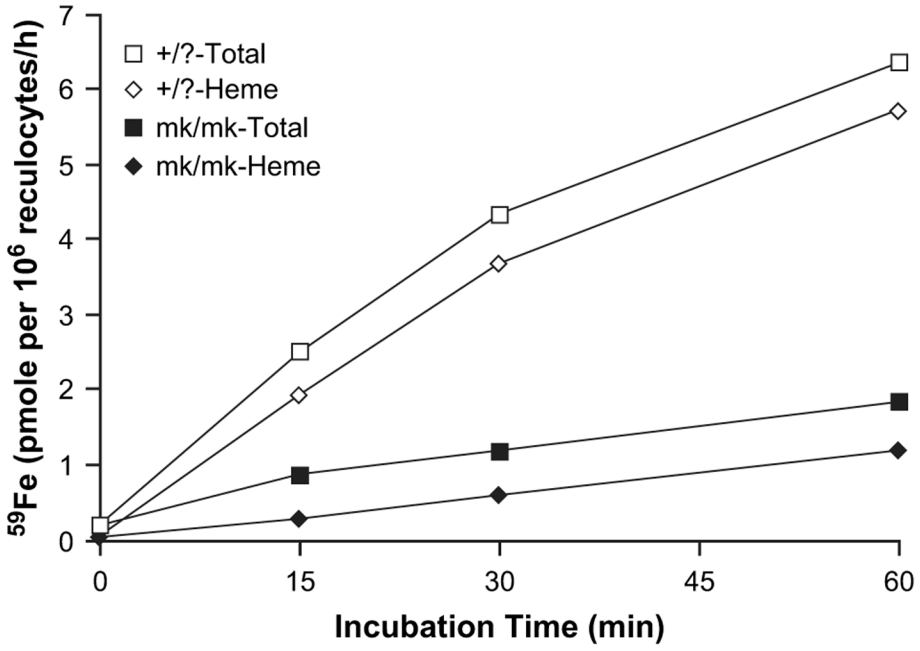

Figure 5.
^{59}Fe uptake from ^{59}Fe-transferrin (Tf) (10 μM) by reticulocytes from *mk/mk* and +/? reticulocytes. ^{59}Fe-heme was extracted using acid methyl ethyl ketone [27].

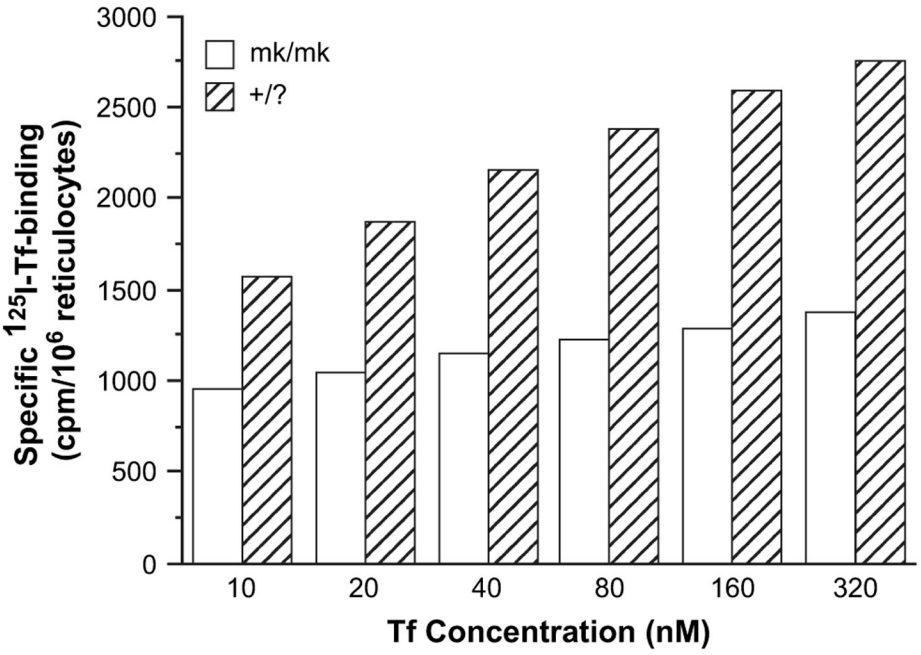

Figure 6.
Specific ^{125}I-transferrin (Tf) binding to membranes of reticulocytes from *mk/mk* and +/? mice.

Table 1

Kinetics of Fe(II) uptake by CHO and CHO-*Nramp2* cells

	Intracellular ^{59}Fe (pmole per 10^6 cells)*					
Time of incubation†	**15 minutes**		**30 minutes**		**60 minutes**	
[Fe(II)]	CHO	CHO-*Nramp2*	CHO	CHO-*Nramp2*	CHO	CHO-*Nramp2*
0.1 μM	0.1	23.0	3.4	45.3	4.4	73.1
1.0 μM	13.1	158.3	21.3	375.5	34.9	716.8
10.0 μM	26.3	288.8	46.8	854.4	102.5	1814.0

CHO = Chinese hamster ovary.

* Indicated values represent averages of duplicates

† pH of the incubation mixture was 5.5.

Table 2

Effects of various divalent metals on Fe(II) uptake*

Metals (μM)	CHO cells	CHO-*Nramp2* cells
Cu^{2+}		
(0.1)	120.5	107.9
(0.5)	153.1	106.9
(1.0)	164.7	109.6
(5.0)	211.1	9.2
(10.0)	230.5	14.2
(50.0)	505.9	25.9
Cd^{2+}		
(10.0)	68.3	42.1
(50.0)	36.6	12.1
Co^{2+}		
(10.0)	91.1	85.4
(50.0)	66.2	47.9
Mn^{2+}		
(10.0)	95.1	92.6
(50.0)	69.4	53.8
(400.0)	30.9	12.5
Ni^{2+}		
(10.0)	99.5	98.4
(50.0)	96.5	80.4
Mg^{2+}		
(10.0)	95.4	93.5
(50.0)	96.1	93.5
Zn^{2+}		
(10.0)	96.2	99.8
(50.0)	99.7	94.9
Pb^{2+}		
(10.0)	213.3	95.0
(50.0)	641.0	120.0

CHO = Chinese hamster ovary.

*Percentages of controls incubated (60 minutes) in the absence of metals.

^{59}Fe(II), 10 μM; ascorbate, 0.44 mM; pH 5.5

Table 3

Effects of various factors on Fe(III) uptake*

Reagent (μM)	**CHO cells**	**CHO-*Nramp2* cells**
Rotenone		
10.0	87.9	46.1
20.0	86.7	58.4
40.0	70.0	52.6
Cu^{2+}		
1.0	94.5	50.2
5.0	91.9	20.6
10.0	76.8	20.2
51.0	71.1	10.4
100.0	48.3	6.7
$K_3Fe(CN)_6$		
0.5	87.9	46.1
1.0	90.2	26.5
3.3	85.3	30.1
10.0	85.1	25.4
1000.0	59.9	19.9
Ascorbate		
440	1138.7	2826.0

* Percentages of controls incubated (60 minutes) in the absence of reagents.

^{59}Fe(III), 10 μM; citrate, 1 mM; pH 5.5.

Table 4

^{59}Fe uptake from $^{59}Fe_2$-Tf*

	Iron uptake (pmol/10^6 cells/h)		
	Experiment 1†	**Experiment 2†**	**Average**
CHO cells	14.9	12.1	13.5
CHO-*Nramp2* cells	14.1	11.4	12.7

CHO = Chinese hamster ovary; Fe = iron; Tf = transferrin.

*10 μM Tf; 20 μM Fe.

†Indicated values represent averages of duplicates

Table 5

Iron uptake by mouse reticulocytes and erythrocytes

Source of ^{59}Fe	^{59}Fe incorporation (pmoles/10^6 cells/h)			
	Reticulocytes		Mature erythrocytes	
	Total	Heme	Total	Heme
^{59}Fe-Tf (10 μM)	6.5	5.6	0.9	0
^{59}Fe-ascorbate (20 μM)	52.8	4.0	3.6	0